Journal of Applied Polymer Science

Healing of polymeric artificial muscle reinforced ionomer composite by resistive heating

Pengfei Zhang,[1] Ukeamezhim Ayaugbokor,[2] Samuel Ibekwe,[2] Dwayne Jerro,[2] Su-Seng Pang,[3] Patrick Mensah,[2] Guoqiang Li[1,2]

[1]Department of Mechanical & Industrial Engineering, Louisiana State University, Baton Rouge, Louisiana 70803
[2]Department of Mechanical Engineering, Southern University, Baton Rouge, Louisiana 70813
[3]Macau University of Science and Technology, Avenida Wai Long, Taipa, Macau, People's Republic of China
Correspondence to: G. Li (E-mail: lguoqi1@lsu.edu)

ABSTRACT: In this study, structural-scale crack healing of artificial muscle reinforced ionomer composite was investigated following the close-then-heal (CTH) healing strategy. Structural-scale crack of 3 mm deep and 1 mm wide in notched beam specimens was first closed by actuation of the embedded polymeric artificial muscles made of fishing lines, followed by intrinsic healing of the ionomer matrix. The healing process was triggered by resistive heating of embedded carbon fibers by DC power. It is found that, with 0.7% by volume of polymeric artificial muscles, the wide-opened cracks are effectively closed, and the closed cracks in the ionomer composite are effectively and repeatedly healed, with a healing efficiency of over 80%. © 2016 Wiley Periodicals, Inc. J. Appl. Polym. Sci. **2016**, *133*, 43660.

KEYWORDS: biomimetic; composites; functionalization of polymers

Received 9 December 2015; accepted 20 March 2016
DOI: 10.1002/app.43660

INTRODUCTION

Healing of polymeric composite was proposed as a way to heal visible and/or invisible cracks for enhancing and hence prolonging the service life of polymeric components.[1] While visible cracks can be repaired comparatively easily, invisible crack such as delamination in laminated composites is difficult to access and repair. Accordingly, active polymeric materials incorporating crack healing functionality have attracted more and more attention throughout academic and industrial communities.[2–8] For extrinsic healing, which is assisted by incorporation of healing agent, either liquid resin delivery systems or solid healing agent per the close-then-heal (CTH) strategy have been proven to be efficient as they can lead to good functionality restoration.[8–15] The delivery systems for liquid healing agent utilize various nano-/micro-/macro-containers such as capsules, hollow fibers, and vascular networks. Upon the creation of a fracture, the healing agent is released with the fracture of the container shell. The agent then fills in the cracks through capillary action. In the close-then-heal system,[8] crack healing process of composite materials mimics biological nature such that it occurs in four different stages: (1) sensing of damage through change in physical properties of the material in the form of cracks, (2) narrowing until closing of the detected cracks by inherent actuator, (3) distribution of the necessary healing agents to the affected area of the material, and (4) gluing the closed crack surfaces to restore its initial physical/mechanical properties. The inherent actuator can be polymeric artificial muscle,[14] or shape memory polymer fiber,[12–16] or shape memory polymer matrix,[17,18] or shape memory alloy wire.[19,20]

Zhang and Li have investigated a healing-on-demand epoxy composite by embedding polymeric artificial muscles and thermoplastic particles.[14] The polymeric artificial muscle was made of polyethylene copolymer fishing line due to its large thermal actuation and lower cost.[21] The thermoplastic particles were used as a solid healing agent. Upon thermal treatment, bending damage induced crack in the epoxy composite was closed by the artificial muscle due to the thermal actuation and healed by the molten thermoplastic particles. The thermal contraction of the artificial muscle is due to the torsional actuation of the twisted then coiled polymer fiber, and such thermally triggered torsional actuation is attributed to both the contraction in axial direction and expansion in transverse direction of the precursor fiber. The kinematic perspective behind the contraction phenomenon has been elaborated by using Love's equation and Van der Heijdgen's theory.[22,23] It has been proved that the epoxy composite could perform repeated crack healing even under constrained boundary conditions, due to the efficient crack closing ability of the continuous artificial muscles.

Ionomer is well-known for its intrinsic healing properties.[24,25] It can be controlled by the change in ionic content through

neutralization with different metallic ions. The healing mechanism in ionomers has been studied, for example, by ballistic impact test on Surlyn 8920 and 8940. It was concluded that the presence of ionic clusters and order-disorder transition are the main mechanism for crack healing.[24] It was pointed out that the healing could occur if sufficient energy (e.g., impact energy or thermal energy) was transferred to the ionomer, heating the material above the order-disorder transition temperature and disordering the ionic aggregates. In short, ionic groups lose their attractions and the molecular chains move around freely when heated. The molecular chains move randomly by crossing the contacted wet surface when fractured surfaces were brought in contact, leading to the crack healing after cooling down. However, it is well known that the elastic rebound is the mechanism for crack closing under ballistic impact. For low strain rate damage, there may not have sufficient rebound to bring the fracture surfaces in contact and healing is impossible. Therefore, as indicted by Li,[8] crack closing through actuation is necessary.

In this study, structural-scale crack healing in ionomer matrix was studied by embedding low-cost polymeric artificial muscles. Carbon fiber was also embedded to serve as an electrical conductor so that crack healing can be triggered by resistive heating. Notched beam specimens were used to investigate the healing efficiency of the composite. Repeated cracking-healing was conducted to evaluate the repeatability of the healing.

EXPERIMENTAL

Raw Materials

Nylon 6 monofilament fishing line (Berkley Trilene XT) and carbon fiber are used as the reinforcement while DuPont Surlyn 8940 ionomeric polymer serves as the matrix. DuPont Surlyn 8940 ionomer is a commercial ethylene methacylic acid (EMAA) based copolymer in which the MAA groups are partially neutralized with sodium ions. Acrylic conforming coating agent MS-475C is used in coating the carbon fibers to provide better bonding with the matrix after the molding process. The coating provides abrasion resistant and as such, excellent electrical insulation against high voltage arcing and corona shorts.

Nylon 6 Artificial Muscle Preparation

Nylon 6 monofilament fishing line has a diameter of 0.46 mm. The twist insertion into the fishing line was accomplished by attaching a 369 g weight to the bottom end of the fishing line. The upper end was fixed to a shaft of a manually controlled rotor. While running the rotor, the attached weight was tethered so as not to rotate, leading to the addition of twists to the fiber.

The effective length of the fishing line is 900 mm.[26] Once the twist insertion comes to a certain level, the fiber coils. The coiled fishing line has a length of 152.4 mm with a diameter of 2 mm. The coiled configuration was then placed in an oven at 130 °C while both ends are clamped. After annealing for 90 min, the polymer artificial muscle made of fishing line yields a spring index of 3.2.

Thermal Properties Characterization

The thermal properties of DuPont Surlyn 8940 ionomer and Nylon 6 monofilament fishing line were investigated using differential scanning calorimetry (PerkinElmer DSC 4000, Waltham MA, USA). The purge gas used is Nitrogen at a gas purge rate of 30 ml min^{-1}. For both materials, they were cooled from 30 °C to −70 °C at a rate of 15 °C min^{-1} and subsequently heated up from −70 °C to 250 °C at a rate of 15 °C min^{-1}. Two cooling and heating cycles were performed on both samples and the second heating cycle was used to determine the glass transition temperature (T_g).

Fabrication of Composite Specimens

A total of two groups of specimens were fabricated. Group 1 was ionomer matrix only which serves as the control. Group 2 was the ionomer composite with reinforcement, which contains both carbon fiber and polymeric artificial muscle.

Pins were nailed down to a wooden mold along the edge length of 254 mm, as shown in Figure 1. A Teflon sheet was placed on the wooden mold to help in demolding. A layer of Surlyn 8940 was first placed on the mold to ensure that the carbon fibers would not be pushed down to the bottom of the composite but well embedded within the matrix during the molding process. In order to increase the heating efficiency by carbon fibers, the carbon fibers were arranged in a grid skeleton. The carbon fiber grid skeleton was then prepared using a dry weaving process.[27] The bay area of the orthogrid skeleton was 12.7 mm × 12.7 mm, indicating 12.7 mm space between two neighboring nails. The artificial muscle was stretched with a 45% prestrain to cover the space between two nails. DuPont Surlyn 8940 pellets were then added to the mold. The composite was fabricated by compressing pellets using melt press (Carver Model 2697), which operated at 120 °C with a compressing pressure of 0.024 MPa. The total compression time was 1 h. When the mold was cooled down, an ionomer composite panel with 12.7 mm thickness was obtained. It is worth noting that Group 1 specimens, which serve as control samples, have the same thickness of 12.7 mm. For Group 2, the volume fraction of the carbon fiber was 10%; and 0.7% by volume of polymeric artificial muscle was used.

Dynamic Mechanical Analysis (DMA) on Polymeric Artificial Muscle

It is necessary to study the thermal actuation behavior of the artificial muscle after the hot press molding under 120 °C. The artificial muscle was tested by a dynamic mechanical analysis (DMA) device (TA Q800). It was first stretched to 45% by the DMA per the iso-strain method, leading to a stretching force of 1.4 N. It was then held under 120 °C for 1 h. After this process, the force was relaxed to 1.1 N. This is to simulate the composite molding process. Following this, the temperature was cooled to room temperature. The test method was then changed to the DMA controlled force method. The force was set to 0.5 N, which is equivalent to 3.05 MPa in the artificial muscle. Cyclic thermal treatment (i.e., heating and cooling) was then performed with the same rate for heating and cooling at 10 °C min^{-1}. The lower bound (T_L) was 20 °C and the higher bound (T_H) was 120 °C.

Three-Point Bending Test

The geometry of the specimen for three-point bending test is shown in Figure 2. A notch was created via ASTM D790 by a razor cut, which was a = 3 mm deep and 1 mm opening. The geometrical dimensions of the beam have a span length s

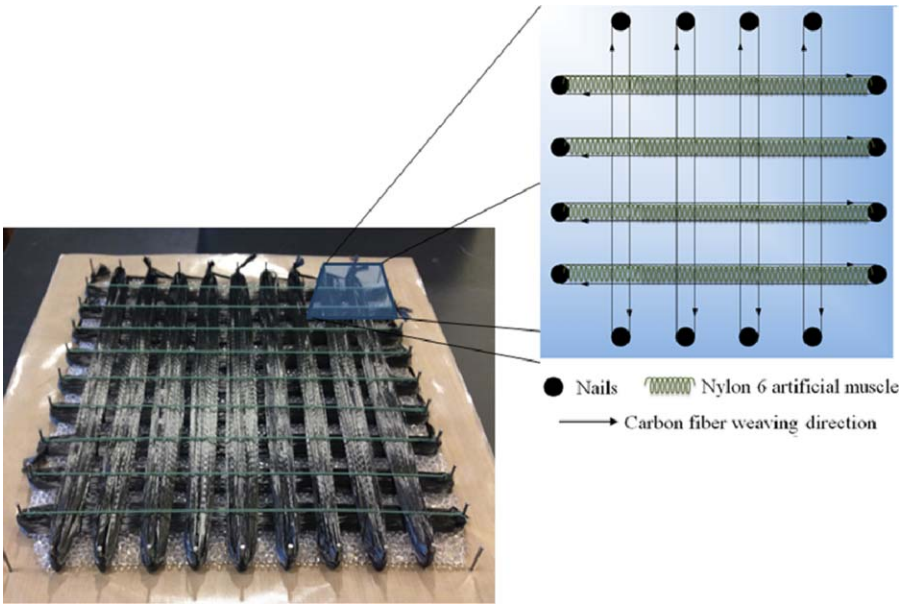

Figure 1. Schematic of mold preparation and ionomer composite fabrication. The enlarged area shows the winding pattern. [Color figure can be viewed in the online issue, which is available at wileyonlinelibrary.com.]

=116 mm, width w = 25.4 mm, and thickness t = 12.7 mm. The test specimen was put on a Material Testing System (MTS) machine (RT/5, MTS) for three-point bending test with a loading rate of 4 mm min^{-1}. The test was run until the material reached peak load, as evidenced by the appearance of a post-peak descending branch. Three effective specimens were tested for each group of samples.

Resistive Heating and Crack Healing

The electrical current flowing through the carbon fiber was used in this study to generate heat from joule heating, which in turn would be transferred to the surrounding ionomer matrix. The crack healing behavior of the ionomer composite after the 3-point bending test was investigated through the resistive heating on carbon fibers. The DC power was provided by a device of TENMA Laboratory DC Power Supply 72-6615. Three current levels were tested, which were 150 mA, 200 mA, and 250 mA, respectively. The temperature was monitored by a thermocouple and recorded by EasyLog software.

In order to measure the electrical resistance of the carbon fiber reinforced ionomer composite specimen, the carbon fibers were exposed on both specimen ends as a conductor. By using a TENMA 72-1015 multimeter digital (bench 3-3/4 digit) device, the electrical resistance was measured as 3.7 Ω. In this study, once the maximum load/deflection was reached on each of the test specimens, resistive heating was conducted to heal the cracks. The setup is shown in Figure 3. The MTS upper crosshead was not allowed to return back to its original position when the peak load during bending test was reached. This simulated a constrained boundary condition to the specimen. The MTS probe (i.e., metal rod providing bending force as shown in Figure 2 as P) was ensured to touch the test specimen without applying any force, as evidenced by a zero reading on the load cell immediately before the healing process. It took about 600 s to heat and heal the specimens. Such damage-healing process was repeated twice.

Morphology Characterization

The fracture healing process of the specimens used for this experimental investigation was observed using a high-resolution Sony XCDCR90CCD camera. The camera has a resolution of 3.7 by 3.7 μm $pixel^{-1}$, and it is equipped with a light source, a control box, and a data communications box, which connected the camera to a computer. The scanning electron microscope (SEM) fractography was also used to study the fracture surface

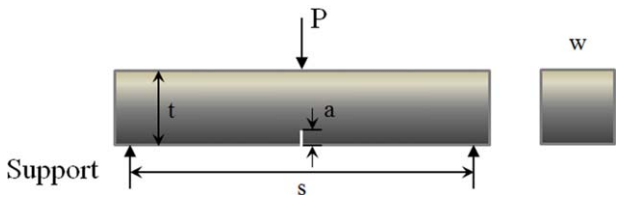

Figure 2. Geometry of specimen for three-point bending test. S is the span length, t is the beam height, W is the beam width, a is the depth of the notch, and P is the bending load. [Color figure can be viewed in the online issue, which is available at wileyonlinelibrary.com.]

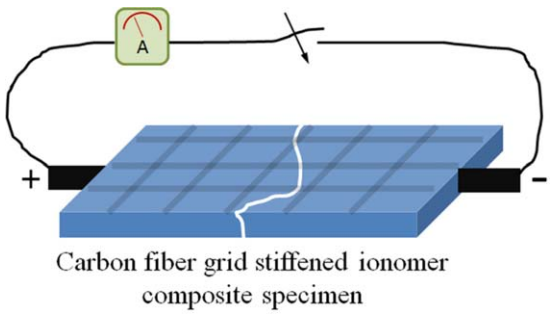

Figure 3. Resistive heating setup for crack healing of carbon fiber grid and artificial muscle stiffened ionomer composite. [Color figure can be viewed in the online issue, which is available at wileyonlinelibrary.com.]

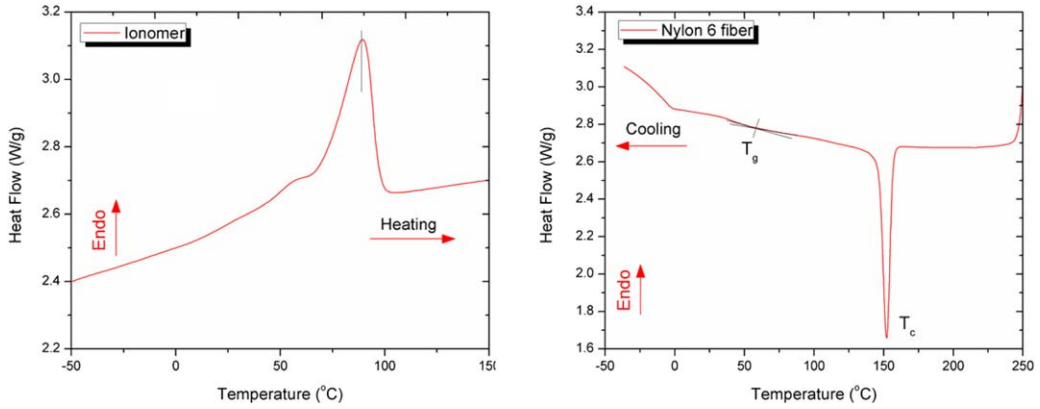

Figure 4. Thermal properties of ionomer from the healing curve (left) and Nylon 6 monofilament fishing line from the cooling curve (right). The melting temperature of the ionomer matrix is about 89.5 °C. The glass transition temperature of the Nylon 6 fiber is 58.4 °C and the crystallization temperature is 152 °C. [Color figure can be viewed in the online issue, which is available at wileyonlinelibrary.com.]

and the bonding surface on the composite. The model used was the Quanta 3D FEG field-emission electron microscope. The specimens were cut into smaller samples, which contained the cracks. After being coated with platinum, the samples were placed onto a sample holder using a two-sided tape and placed into the SEM chamber for characterization.

RESULTS AND DISCUSSION

Differential Scanning Calorimetry (DSC)

As shown in Figure 4, the thermal properties of the ionomer (left) and Nylon 6 monofilament fishing line (right) have been plotted according to the differential scanning calorimetry (DSC) test. The heat flow curve for ionomer shows a peak at 89.5 °C, which represent the melting temperature (T_m). Since the matrix was made of ionomer, the triggering temperature for crack healing should be at least higher than its melting temperature (i.e., 89.5 °C). The other curve for Nylon 6 monofilament fishing line shows a single glass transition temperature at 58.4 °C and crystallization temperature at 152 °C.[28,29] And the melting temperature of the Nylon 6 fishing line is at 192.3 °C when examining the heating curve from the DSC results, which is not plotted here. In this study, the polymeric artificial muscle was annealed at a temperature 130 °C, i.e., in-between the glass transition and melting transition.

Resistive Heating

The electrical resistance of the carbon fiber was 3.7 Ω. The resistive heating was shown in Figure 5, which was under the DC current 150 mA, 200 mA, and 250 mA, respectively. It shows that the temperature was stabilized within 1 min. In the case of 150 mA, the stabilized temperature was about 80 °C; and it was about 128 °C for 200 mA, but 170 °C for 250 mA. In this study, the electrical current-induced heat was expected for both triggering artificial muscle contraction (i.e., leading to crack close) and melting ionomer with the aim of wetting fracture surface, leading to crack healing.[30] Notice that, the melting point of the ionomer matrix is 89.5 °C. It is found out that once the local temperature through the resistive healing is higher than 130 °C, the heat dissipates in the ionomer matrix

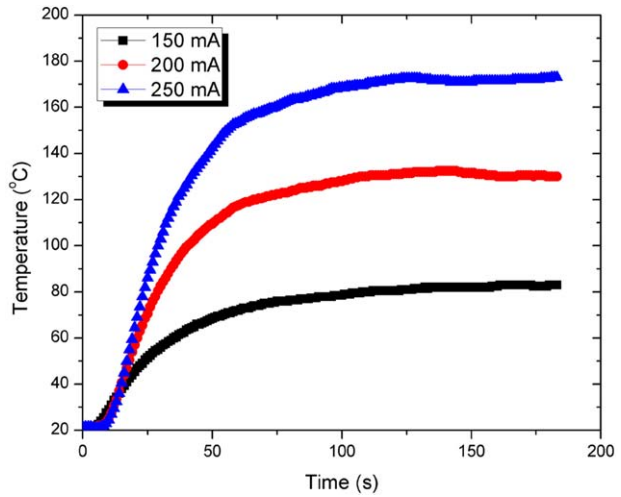

Figure 5. Temperature change with resistive heating time by DC currents at 150 mA, 200 mA, and 250 mA. The increase in temperature is seen as the current increases initially, and stabilizes as time goes by. [Color figure can be viewed in the online issue, which is available at wileyonlinelibrary.com.]

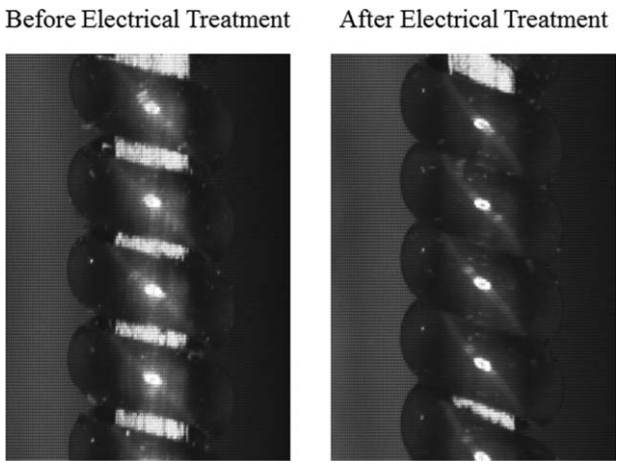

Figure 6. Nylon 6 artificial muscle under 100 gram load (left) and thermal contraction of the muscle under electrical current at 200 mA. The contact between the coils in the right figure indicates contraction of the muscle.

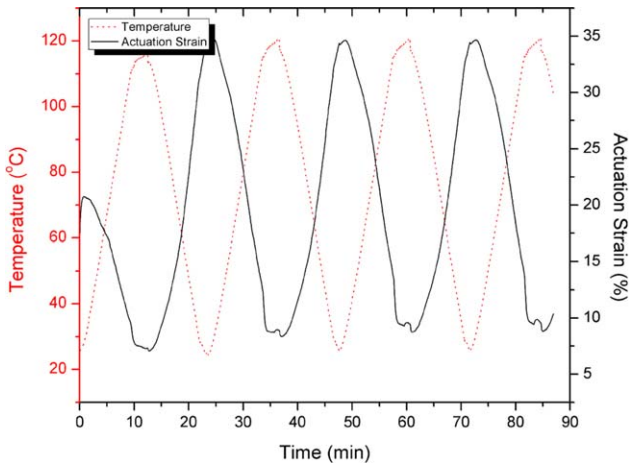

Figure 7. Thermal actuation strain of Nylon 6 artificial muscle along with temperature change under 3.05 MPa applied stress. The dotted line is temperature and the solid line is the actuation strain. It shows cooling induced elongation and heating induced contraction. [Color figure can be viewed in the online issue, which is available at wileyonlinelibrary.com.]

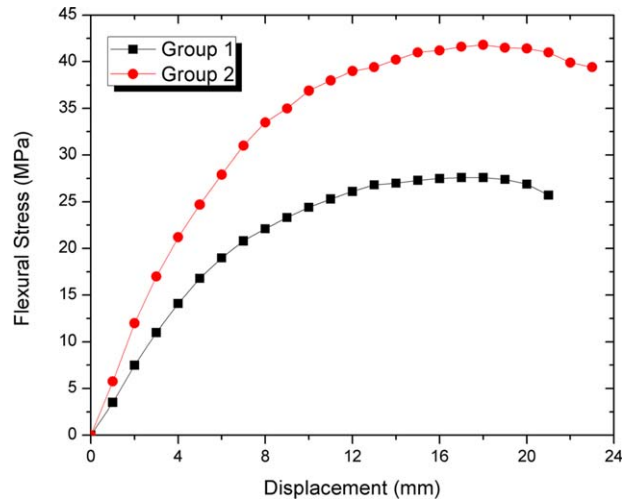

Figure 8. The comparison between the three-point bending test results of ionomer composite specimens without initial notch. Group 2 specimen shows lowered bending strength. [Color figure can be viewed in the online issue, which is available at wileyonlinelibrary.com.]

quickly, resulting in failure of the structure in a few minutes. In this study, 200 mA was chosen to heat the carbon fiber during healing because it led to the stabilized temperature that caused ionomer melting and muscle actuation, without overheating the ionomer matrix.

Thermal Actuation of Nylon 6 Artificial Muscle

The muscle contraction under electrical current-induced heat was studied by inserting carbon fiber into the muscle as mandrel, as shown in Figure 6. The polymeric artificial muscle with spring index of 3.2 was prepared in advance. A bundle of carbon fiber was inserted through the muscle coils, as shown in Figure 6 (left). Under 100 gram external load (equivalent to 5.82 MPa when normalized to the fiber cross-section area), the artificial muscle was stretched, leading to coil separation. A DC power current 200 mA was provided through the carbon fiber, which generated heat along the carbon fiber bundle, leading to thermal contraction within 20 s, as shown in Figure 6 (right). Such electrical induced contraction was expected to narrow and close cracks for the healing purpose in this study.

One of the concerns for Nylon 6 artificial muscle based crack healing composite is the loss of thermal contraction after hot press molding at 120 °C for 1 h. In order to verify its contraction performance, the polymeric artificial muscle was stretched to 45% prestrain and held for 1 h at 120 °C. After that, the constraint load was removed. Once being cooled down, an external load (about 3.05 MPa) was provided to the muscle, leading to about 22.5% prestrain, as shown in Figure 7. During the heating cycle, the muscle contracted to about 7% at 120 °C. When cooling down to 20 °C, the muscle was stretched to 35% due to the external load. In the second heating cycle, the muscle contracted to about 8%. The stroke can be as high as 27% (i.e., 35% – 8% = 27%), with an actuation ratio of 77%. The actuation ratio is defined as stroke (i.e., 27%) over strain (i.e., 35%) at higher temperature during heating. It is similar to the shape recovery ratio, that is, if the ratio approaches 100%, it indicates that the muscle could contract back to its initial configuration.[8] The thermal actuation and load-induced stretching were repeated for three times along with heating and cooling cycles. It shows no actuation ratio loss even after multiple cycles. As compared, this polymeric artificial muscle has higher stroke than any other types, such as Polyethylene copolymer artificial muscle,[14] Nylon 6,6 artificial muscle and even Nylon 6 artificial muscle prepared

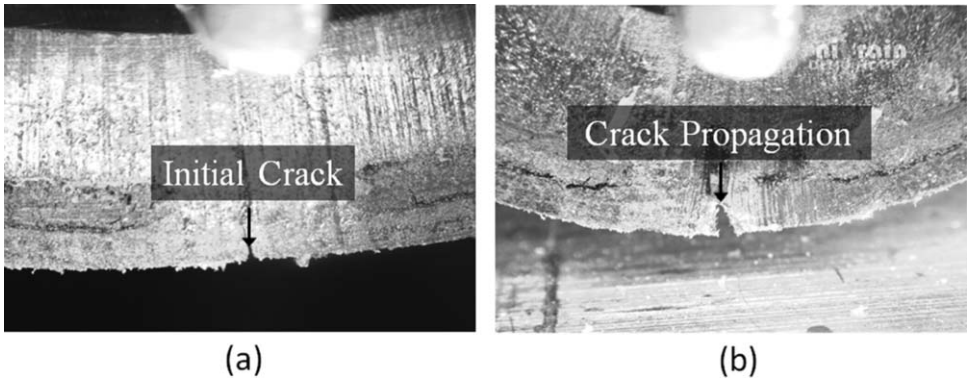

Figure 9. Group 2 specimen (a) initial notch by a razor cut, and (b) crack propagation during the bending test.

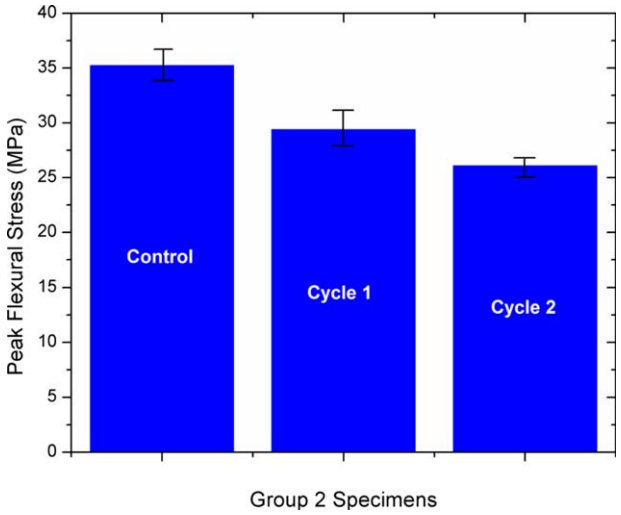

Figure 10. Peak flexural stresses of three-point bending test for carbon fiber grid and artificial muscle stiffened ionomer composite beam. It shows that the bending strength is not fully recovered and the strength further reduces as the damage-healing cycle increases. [Color figure can be viewed in the online issue, which is available at wileyonlinelibrary.com.]

by Haines *et al.*[21] This indicates that the spring index effect is significant.

Three-Point Flexural Test

ASTM D 790 was used to determine the flexural property of the ionomer composites. Group 1 and Group 2 specimens were tested under three-point bending. Both of them were first bended without initial notch, to establish the baseline bending strength. This is also to investigate the effects of carbon fiber and artificial muscle reinforcement on flexural properties. Figure 8 shows a typical result of the flexural property under three-point bending. It shows that their failure displacements do not vary too much; but the peak flexural stresses have been improved by the carbon fiber grid skeleton and artificial muscle reinforcement as compared with the control specimen, which is 27.5 ± 1.6 MPa. The peak stress of Group 2 is 42.1 ± 2.3 MPa, leading to the flexural strength improvement ratio up to about 53%. As can be seen from the curve, the flexural stresses increases first and then decrease gradually as time passes by, rather than dropping abruptly to small value. This is due to the high toughness of the ionomer matrix. The flexural strength was recorded from the peak value on the curve.

Crack Healing and Repeatability

Three-point bending was utilized here to further propagate the initial notch in the composite specimens. Figure 9 shows the initial crack before bending test and crack propagation under bending load. The peak flexural stress was calculated based on the test results according to ASTM D 790. As shown in Figure 10, the control specimens are the notched Group 2 specimens without crack propagation/healing history. The cycle 1 and cycle 2 are the bending test after the first healing cycle and second healing cycle, respectively.

Crack healing efficiency is determined by σ_i/σ_o, where σ_i is the peak flexural stress after crack healing event, $i = 1$, 2, and σ_o is the peak stress of the control specimen in Figure 10. A can be seen, resistive heating can trigger the healing process efficiently. The healing efficiency in the first healing cycle is $86 \pm 2\%$; then it becomes $78 \pm 5\%$ in the second healing event. Figure 11 shows that the crack was significantly narrowed by artificial muscle and shape memory behavior of the ionomer matrix as compared with Group 1 specimen. Obviously, it can be observed that the bending-induced crack could be closed and healed for multiple times by the artificial muscle for crack closing and the ionomer matrix for intrinsic healing. For the Group 1 specimens, the crack is still wide opened and thus healing is not achieved. However, the healed sample still leaves with a narrowed scar on the healing zone. Probably this is why the healing efficiency could not reach 100%.

CONCLUSIONS

In this study, crack healing behavior of artificial muscle reinforced ionomer composite was investigated under DC power supply. It shows that the reinforcement by artificial muscle and carbon fiber grid has improved the flexural strength up to 53%

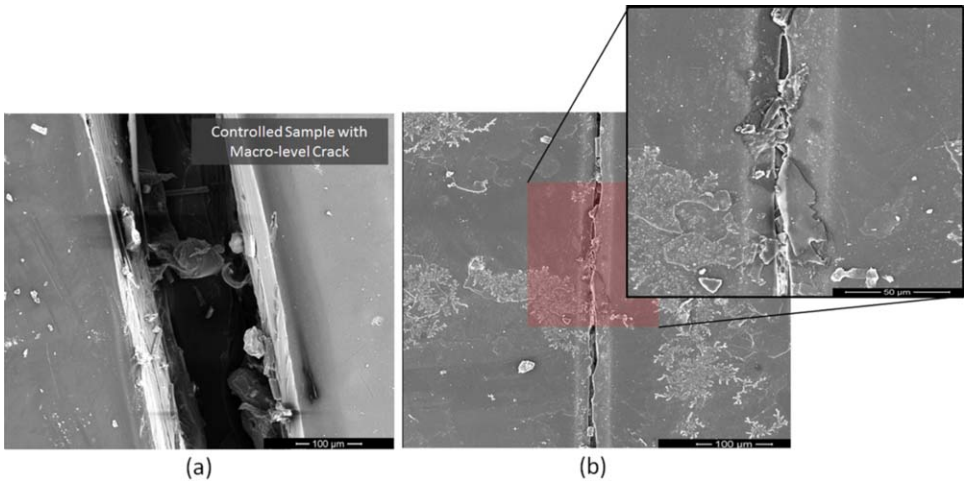

Figure 11. SEM results showing crack healing performance of (a) Group 1 sample and (b) Group 2 sample. It is clear that the crack in the Group 2 specimen has been significantly narrowed. [Color figure can be viewed in the online issue, which is available at wileyonlinelibrary.com.]

in terms of bending strength. With the help of carbon fiber grid, it took about 60 s to reach the actuation temperature when applied with resistive heating. The cracking/healing performance indicates that such an ionomer composite can heal structural scale cracks efficiently, timely, and repeatedly under constrained boundary condition, without the need for external healing agent.

ACKNOWLEDGMENTS

This study was financially supported by National Science Foundation under grant number CMMI 1333997, the Cooperative Agreement NNX11AM17A between NASA and the Louisiana Board of Regents under contract NASA/LEQSF(2011-14)-Phase3-05, and Army Research Office under grant number W911NF-13-1-0145. The assistance by Qianxi Yang, Jizhou Fan, and Lu Lu is greatly appreciated.

REFERENCES

1. Zhang, P.; Li, G. *Prog. Polym. Sci.* **2015**. DOI: 10.1016/j.progpolymsci.2015.11.005.
2. Yuan, Y.; Yin, T.; Rong, M.; Zhang, M. *Polym. Lett.* **2008**, *2*, 238.
3. Blaiszik, B.; Kramer, S.; Olugebefola, S.; Moore, J. S.; Sottos, N. R.; White, S. R. *Annu. Rev. Mater. Res.* **2010**, *40*, 179.
4. Wu, D. Y.; Meure, S.; Solomon, D. *Prog. Polym. Sci.* **2008**, *33*, 479.
5. Thakur, V. K.; Kessler, M. R. *Polymer* **2015**, *69*, 369.
6. Zhu, D. Y.; Rong, M. Z.; Zhang, M. Q. *Prog. Polym. Sci.* **2015**, *49–50*, 175.
7. Yang, Y.; Ding, X.; Urban, M. W. *Prog. Polym. Sci.* **2015**, *49–50*, 34.
8. Li, G. Self-Healing Composites: Shape Memory Polymer Based Structures; Wiley: West Sussex, **2014**.
9. White, S. R.; Sottos, N.; Geubelle, P.; Moore, J.; Kessler, M. R.; Sriram, S.; Brown, E. N.; Viswanathan, S. *Nature* **2001**, *409*, 794.
10. Trask, R.; Bond, I. *Smart Mater. Struct.* **2006**, *15*, 704.
11. Hamilton, A. R.; Sottos, N. R.; White, S. R. *Adv. Mater.* **2010**, *22*, 5159.
12. Li, G.; Zhang, P. *Polymer* **2013**, *54*, 5075.
13. Zhang, P.; Li, G. *J. Polym. Sci. B: Polym. Phys.* **2013**, *51*, 966.
14. Zhang, P.; Li, G. *Polymer* **2015**, *64*, 29.
15. Li, G.; Meng, H.; Hu, J. *J. R. Soc. Interface* **2012**, *9*, 3279.
16. Li, G.; Ajisafe, O.; Meng, H. *Polymer* **2013**, *54*, 920.
17. Nji, J.; Li, G. *Polymer* **2010**, *51*, 6021.
18. Nji, J.; Li, G. *Smart Mater. Struct.* **2010**, *19*, 035007/1–9.
19. Kirkby, E. L.; Rule, J. D.; Michaud, V. J.; Sottos, N. R.; White, S. R.; Manson, J. *AE. Adv. Funct. Mater.* **2008**, *18*, 2253.
20. Kirkby, E. L.; Michaud, V. J.; Manson, J. A. E.; Sottos, N. R.; White, S. R. *Polymer* **2009**, *50*, 5533.
21. Haines, C. S.; Lima, M. D.; Li, N.; Spinks, G. M.; Foroughi, J.; Madden, J. D.; Kim, S. H.; Fang, S.; de Andrade, M. J.; Göktepe, F.; Göktepe, Ö.; Mirvakili, S. M.; Naficy, S.; Lepró, X.; Oh, J.; Kozlov, M. E.; Kim, S. J.; Xu, X.; Swedlove, B. J.; Wallace, G. G.; Baughman, R. H. *Science* **2014**, *343*, 868.
22. Love, A. A Treatise on the Mathematical Theory of Elasticity; Dover Publication: New York, **1944**.
23. Van der Heijden, G.; Thompson, J. *Nonlinear Dyn.* **2000**, *21*, 71.
24. Fall, R. A. M.S. Thesis, Virginia Polytechnic Institute and State University, Blacksburg, VA, **2001**.
25. Ghosh, S. K. Self-Healing Materials: Fundamentals, Design Strategies, and Applications; Kalista, S. J., Ed.;Wiley-VCH: Weinheim, **2009**; Chapter 3, pp 73–90.
26. Zhang, P. Ph.D. Dissertation, Louisiana State University, Baton Rouge, LA, **2015**.
27. Li, G.; John, M. *Compos. Sci. Technol.* **2008**, *68*, 3337.
28. Forster, M. J. *Text. Res. J.* **1968**, *38*, 474.
29. Greco, R.; Nicolais, L. *Polymer* **1976**, *17*, 1049.
30. Wool, R.; O'connor, K. *J. Appl. Phys.* **1981**, *52*, 5953.